Antibacterial activity of the root extracts of *Garcinia Kola* against MDR *Staphylococcus aureus :* Invitro and insilico studies.

Abdulbasit Haliru YAKUBU[1] and Muhammad Mustapha MUHAMMAD[2]

1. **Department of Pharmaceutical Chemistry, Faculty of Pharmacy, PMB 1069, University of Maiduguri, Maiduguri, Borno, Nigeria.**
2. **North East Biotechnology Center, PMB 1069, University of Maiduguri, Maiduguri, Borno, Nigeria.**

Corresponding author mail: pharmahy071@gmail.com

Abstract

MDR ***Staphylococcus aureus*** is an important bacteria with clinical and economic implication. Plants including Garcinia kola provides bioactive principles with diverse structural and biological features.. The n-Butanol fraction of *G.kola* root extract recorded the highest activity against MDR staph aureus (18.50±0.41) compared to the chloroform (10.00±2.12) and methanol (8.166±0.62) extarct, with no activity recorded with the n-Hexane extract. Analysis of this fraction on GC-MS recorded 14 phytoconstituents with varying structural composition; containing important scaffolds & motifs of benzoquinone, imidazo[1,2-a]pyridine, Chlorocarbazole and azetidine that present key pharmaceuticals as antibiotic and for drug development. Further inslico molecular docking studies of these compounds on antibacterial drug target; Tyrosyl-tRNA synthetase (PDB 1JIJ) from MDR staph aureus was documented. 9 compounds (CID_619544, CID_619583, CID_5732, CID_616643, CID_622021, CID_ 616496, CID_590350, CID_16486 and CID_66747) had good binding scores ranging from -4.63 to -7.08 kcal/mol; with CID_590350 having the highest score. The compounds formed various bonding with the 1JIJ amino acid residues including H-bond, van der waal and π interactions. CID_16486 and CID_66747 bind to the most active binding pocket (Drug score: 0.82 &0.72) while CID_619583 tend to bind outside the active binding pocket. They also have good pharmacokinetic and toxicity profile. Therefore, these compounds are considered as suitable prospective antibiotics against MDR ***Staphylococcus aureus*** after successful *invitro* and *insilico* experimental validation.

Key words: Garcinia kola, Antibacterial, MDR *Staphylococcus aureus*, tyrosyl-tRNA synthetase (YRS), Molecular docking.

INTRODUCTION

In the past decades, there had been an alarming increase in the rise of antimicrobial resistance. This purse a serious public health concern as choice of clinical drugs become limited and ineffective. This in turn, results to negative clinical and economic consequences on patient's health, increase in nosocomial infection, prolonged hospital stay and mortality. The mortality due to this infections is projected to be over a 10million by 2050 (Ferdes, 2018). This prompt the call for global advocacy campaign in antibiotic stewardship.

Among the common encountered bacteria of clinical importance is *Staphylococcus aureus. It's the* most common cause of nosocomial infections, bacteremia and is a bacterial pathogen with high propensity to develop antibiotic resistance (Steinig *et al*., 2019 and kot *et al*., 2020). The methicillin resistance *Staph. aureus* MRSA confers its resistance to β-lactam antibiotic by acquiring the genetic element; *staphylococcal* cassette chromosome mec, which carries the *mecA* gene and also of the new variant mecC (Kot *et al*., 2020). This MRSA later become resistant to other class of antibiotic including broad spectrums by acquiring new antimicrobial resistance elements and are termed Multidrug Resistant MDR MRSA (Kot *et al*., 2020). Hiramatsu and colleagues described the genetic basis of the ability of *Staph. aureus* to acquire multi-antibiotic resistance (Hiramatsu *et al*., 2014). This MDR MRSA presents serious challenges in the treatment and control of *Staph. aureus* infections; standard clinical agents used in its treatment include vancomycin, linezolid, daptomycin, tigecycline, telavancin, and ceftaroline (Anstead *et al*., 2013 and kot *et al*., 2020).

Aminoacyl-tRNA synthetases (AARSs) are key important enzyme that are involved in bacterial transcription, translation and signalling pathways. They catalyse the covalent binding of relevant amino acid with specific tRNA. Tyrosyl-tRNA synthetase (TyrRS) is a class I synthetases and because of their role in protein synthesis, inhibitors of this enzymes are been explored for the discovery and development of potential new antibiotic agents (Qiu *et al*., 2019 and Farshadfar *et al*., 2020)

Plant parts had been in use since genesis for the treatment of various ailments. They are characterized by their large structural and diverse chemical entities known as secondary metabolites, which presents unique bioactive principles with elaborate biological activities (Ferdes, 2018 and Othman *et al*., 2019). Plant phytochemicals had been explored and

documented for their potential antibacterial activity against sensitive and resistant pathogens (Khamenah *et al*., 2019).

Among the Plant species explored for its antibacterial activity is Garcina kola, popularly known as bitter kola. It's a perennial crop that belongs to the *Guttiferae* family. This plant had been utilized among locals for its medicinal importance. A review of its ethnobotanical, phytochemistry, pharmacological & toxicological, and therapeutic properties had been documented (Bubu *et al*., 2016 and Oliver *et al*., 2016).

A plethora of literature's emerged on the antibacterial activity of *G.kola* especially the seed and leave part. However, there's scarce research on the antibacterial activity of the root part of *G.kola* and activity of the plant on MDR *staph aureus.*

With the increase in antibiotic resistance and limited availability of new drug entry for possible clinical use against MDR *staph aureus*, it's imperative for the research on new bioactive principles against this organism.

In this study, we undertook the antibacterial studies of the root extracts (n-Hexane, n-Butanol, chloroform, and methanol) of *G.kola* against isolated MDR *Staph. aureus*, as well as carrying out *insilico* molecular docking studies of the phytoconstituents from the active extract against Tyrosyl-tRNA synthetase.

MATERIALS AND METHOD.

Plant Collection and Identification

Fresh root parts of *G.kola* was collected aseptically in October, 2020 from Jos LGA, Plateau State, Nigeria, and identified by a Medicinal Botanist (Mal Namadi Sanusi) of the Biology department, ABU Zaria, Nigeria.

Preparation of Plant Extract and Its Fractions

The method of plant extract preparation employed in this studies was adopted from our previous work with modification (Yakubu *et al*., 2020). In this study, 500mg of the pulverized root sample material was extracted using maceration method with n-Hexane, Chloroform, n-Butanol and Methanol and allowed for 72hrs under room condition. The mixture was filtered with a filter paper and allowed to dry under room temperature to obtain the crude extract; stored in a desiccator, and used further analysis.

Biological Activity

Antimicrobial Assay

Test Organisms

Isolates of MDR *staphylococcus aureus* were obtained from the Microbiology department, University of Maiduguri and were stored at 2-8^{0}C until required.

Preparation of Extract solutions and test organism for Pathogenic Assay.

In this study, we adopt the method we employed in our previous studies (Yakubu *et al*., 2020). A stock solution of 1000mg/ml was prepared and a two-fold serial dilution was carried out to obtain working solutions of varying concentrations.

Test organisms cultured for 24hrs were suspended in a sterile bottle containing pure broth. Normal saline was added gradually and the turbidity was observed and compared to that of 0.5 Mcfarland standard; this was then diluted to produce 10^6cells/mL and used in the experiments. Nutrient agar was prepared accurately to the manufacturer's specification and sterilized at 121^{0}C for 15min which was then allowed to cool to 50^{0}C in a water-bath. The test organism (1mL containing 10^6cells/mL) was inoculated into pre-labeled petri plates (90mm diameter), then 19mL of the molten agar was added to each petri plate, shacked and allowed to set at room temperature on a flat surface (Yakubu *et al*., 2020).

Antimicrobial Susceptibility Assay (agar well diffusion method)

The antibacterial activity of the crude extracts was determined in accordance with the agar-well diffusion method described by Indabawa and Arzai (2011) and Yakubu *et al* (2020). The bacterial isolates were grown for 18 h in a nutrient broth and standardized to 0.5 McFarland standards (10 6 cfuml^{-1}). Two hundred microliter of the standardized cell suspensions were spread on a Mueller-Hinton agar (Oxoid) and wells were bored into the agar using a sterile 6 mm diameter cork borer. Approximately 100 µl of the crude extract at 100, 75, 50 and 25 mgml^{-1} were introduced into the wells, allowed to stand at room temperature for about 2 h and then incubated at 37°C. Controls were set up in parallel using the solvents that were used to reconstitute the extract. After 24h, the plates were observed for the zones of inhibition. The effects were compared with those of Vancomycin at a concentration of 5 mg/ml. Antibacterial activity was evaluated by measuring the diameters of zones of growth inhibition in triplicates and results were presented as Mean±SEM. 00 indicates negative and no effect, diameter < 8.0mm

zone of inhibition indicates low activity, >8mm of inhibition indicates high activity (Indabawa and Arzai, 2011).

GC-MS ANALYSIS

A GC clarus 500 Perkin Elmer system comprising a AOC-20i auto sampler and gas chromatograph interfaced to a mass spectrometer instrument was employed for the Gas column-Mass spectroscopy; operating with a column elite-1 fused silica capillary column (30x0.25 mm IDx1 EM df, composed of 100% dimethyl polysiloxane), electron impact mode at 70 eV; helium (99-999%) was used as carrier gas at a constant flow of 1 ml/min and an injection volume of 0.5 EI (Oludare *et al*., 2018). The oven temperature was programmed from 110º C (isothermal for 2 min) with an increase of 10 C / min, to 200 ºC then 5 º C / min 280 º C, ending with a 9 min isothermal at 280 º C; a scan interval of 0.5s and fragments from 40 to 550 Da.

INSILICO ANALYSIS

Preparation of protein complex

The 3D structure of the protein target *staph. aureus* tyrosyl-tRNA synthatase PDB 1JIJ was retrieved from the protein data bank PDB (Pisano *et al*., 2019). Missing loops were checked for, alternate conformations were removed, bond orders were determined, side chains were optimized and fixed, improper chirality was identified, dissulfide bonds were checked, steric clashes were identified and fixed, protonation states were determined, and the protein where optimized and their energy calculated using a program implemented in SwissPDViewer (v4.1.0) (Isa *et al*., 2018).

Molecular Docking

The most critical requirement for interaction of tyrosyl-tRNA synthatase with the ligands it's the proper orientation and conformation of the ligands in its active sites. Compounds from GC-MS with desirable physicochemical properties were selected and ligands 3D structure where obtained from PubChem. The molecular docking was analysed with AutoDock4.0. The docking analysis was evaluated at a free binding energy of the protein-ligand complex determined with a total of 110 runs, maximum evaluation of 2500,000, maximum generation of 27,000 and with a population size of 150. The dimension of the grid was set at 60×60×60 A with a grid spacing of 0.375 Å. A Lamarckian genetic algorithm was used to compute the free binding energy. The protein-ligand complex was visualized using Ligplot+v.1.4.5 tool (malik *et al*., 2017), Pymol

Molecular Graphics System, Version 1.8 Schrodinger, LLC (DeLano, 2002) and Discovery studio. Prediction of binding site and 2D ligand-protein complex interaction was viewed with DoGSiteScorer and Poseview respectively from Proteins*Plus* sever (Fricker *et al*., 2004; Stierand *et al*., 2006 and Volkamer *et al*., 2012).

Drug Likeness and Pharmacokinetics Analysis

All docked ligands were screened for the Lipinki's rule of five (RO5), pharmacokinetics and toxicity profile using the SwissADME (Daina *et al.,* 2017). ADME/TOX program (Lipinski *et al.,* 2001) and DataWarrior tool (Sander *et al.,* 2015).

RESULTS

Table 1: *Invitro* antimicrobial activity of *G.kola* extracts on *MDR staph aureus*.

	Extract				
Concentration (mg/ml)	**n-Hex**	**$CHCL_3$**	**n-But**	**MeOH**	**Van(5mg/ml)**
100	00.00±0.00	10.00±2.12	18.50±0.41	8.166±0.62	25.00±1.3
75	00.00±0.00	8.83±1.5	13.50±0.40	8.16±0.23	-
50	00.00±0.00	7.50±0.93	11.83±0.85	3.33±0.24	-
25	00.00±0.00	6.33±1.4	11.16±0.62	3.00±0.35	-

Key: n-Hex: n-Hexane n-But: n-Butanol Van: Vancomycin

$CHCL_3$: Chlroform MeOH: methanol

Table2: GC-MS analysis of the n-Butanol crude extract of *G.kola*

S/No	PubChem ID	Compound	Formular	Molecular Weight	Retention Time(min)	Peaks
1	CID_619544	2-Hydroxy-3-(thiophen-2-yl)methyl-5-methoxy-1,4-benzoquinone	$C_{12}H_{10}O_4S$	250	4.02	0
2	CID_619583	9,9-Dichloro-9-silafluorene	$C_{12}H_8Cl_2Si$	250	7.310	0
3	CID_5732	Zolpidem	$C_{19}H_{21}N_3O$	307	7.310	0
4	CID_616643	Pyridazine-3,5-dicarbonitrile, 1,6-dihydro-4-amino-6-imino-1-(2-nitrophenyl)-	C12H7N7O2	281	7.310	0
5	CID_240576	Pyrimidine, 5-bromo-2,4-bis(methylthio)-	$C_6H_7BrN_2S_2$	250	2.956	1
6	CID_622021	5H-Naphtho[1,8-bc]thiophen-5-one, 3,4-dihydro-2-phenyl-	$C_{17}H_{12}OS$	264	7.42	2
7	CID_616496	9,9'-Bis(3,6-dichlorocarbazole)	$C_{24}H_{12}Cl_4N_2$	468	7.42	2
8	CID_590350	3,8-Di-t-butyl-5,6-diphenyl-2,9-dithia-1-phosphabicyclo[4.3.0]nona-3,7-diene 1-sulfide	$C_{26}H_{31}PS_3$	470	7.42	2
9	CID_6586	Methyl chloroformate	$C_2H_3ClO_2$	94	1.708	1
10	CID_24992030 2	Diborane(6), μ-mercapto-	B_2H_6S	60	1.909	2
11	CID_13770	1-Methylcyclopropanemethanol	$C_5H_{10}O$	86	1.909	2
12	CID_16486	(S)-(-)-2-Azetidinecarboxlic acid	$C_4H_7NO_2$	101	2.55	1
13	CID_7983	Butanoic acid, butyl ester	$C_8H_{16}O_2$	144	3.534	2
14	CID_66747	2-Hydroxyethyl benzoate	$C_9H_{10}O_3$	166	3.534	2

Table 3: Physiochemical analysis of constituents from the n-Butanol crude extract of *G.kola*

S/N	PubChem ID	Molecular weight (≤500)	Number of HBA (≤10)	Number of HBD (≤5)	MolLogP (≤5)	Druglikeness
1	CID_619544	250.273	4	1	1.2614	3.7229
2	CID_619583	251.88	0	0	2.7656	-37.314
3	CID_5732	307.396	4	0	2.7975	3.3181
4	CID_616643	281.235	9	2	-0.8212	-6.832
5	CID_240576	251.172	2	0	2.1155	-3.2172
6	CID_622021	264.347	1	0	4.6609	-0.10276
7	CID_616496	470.185	2	0	7.7372	0.95217
8	CID_590350	470.704	0	0	9.3002	-9.1649
9	CID_6586	94.4968	2	0	0.8196	-12.134
10	CID_249920302	-	-	-	-	-
11	CID_13770	86.1334	1	1	0.7001	-7.3666
12	CID_16486	101.105	3	2	-2.9545	-0.55335
13	CID_7983	144.213	2	0	2.3527	-7.6022
14	CID_66747	166.175	3	1	1.0522	-1.6196

Table 4: Docking scores and residues involved in h-bond formation

S/no.	Compound Id	Docking score (kcal/mol)	Residues involve in H-bonds	Distance (Å)
1	CID_619544	-4.63	Thr169 Thr169	2.97 3.02
2	CID_619583	-5.91	0	0
3	CID_5732	-6.30	0	0
4	CID_616643	-5.62	Thr169	2.72
5	CID_240576	-4.33	0	0
6	CID_622021	-7.01	Thr169	3.06
7	CID_616496	-7.00	0	0
8	CID_590350	-7.08	0	0
9	CID_6586	-2.95	Arg183	2.97
10	CID_249920302	-	-	-
11	CID_13770	-3.49	Ser202	2.74
12	CID_16486	-4.64	Lys84 Tyr170 Asp40 Asp80 Arg88	2.67 3.03 2.88 2.98 2.85
13	CID_7983	-4.23	Leu206	2.90
14	CID_66747	-4.93	Glu205	2.99

Table 5: Pharmacokinetic analysis of constituents from the n-Butanol crude extract of *G.kola*

S/no.	Compound name	BBB	CYP2D6 inhibitor	Mutagens	Tumorigens	reproducibility	Irritant
1	CID_619544	no	no	high	none	none	none
2	CID_619583	yes	yes	none	none	none	high
3	CID_5732	Yes	yes	none	none	high	none
4	CID_616643	No	no	none	none	none	none
5	CID_240576	Yes	no	none	none	none	none
6	CID_622021	yes	No	high	none	none	none
7	CID_616496	No	no	low	none	none	none
8	CID_590350	No	no	low	none	none	none
9	CID_6586	Yes	no	high	high	none	low
10	CID_249920302						
11	CID_13770	No	yes	none	none	none	none
12	CID_16486	No	no	none	none	none	None
13	CID_7983	Yes	no	high	none	none	None
14	CID_66747	Yes	no	none	none	high	High

DISCUSSION

G.kola had been evaluated for its antibacterial properties including its activity on *Staph. aureus* . Ajayi *et al* (2014) evaluated the antibacterial activity of the seed extracts of *G.kola* against clinical dental isolates of Staph species. The ethanol extract showed an inhibitory activity of 13 and 14 at 400mg/ml. Similar activity was reported on the seed, bark and root extract on *Staph. aureus* (Akelere *et al*., 2008 and Indabawa and Arzai, 2011 and Ukaoma *et al*., 2013). Results of this study highlighted the inhibitory antimicrobial activity of the different root extract of *G.kola*. Activity was recorded in the $CHCl_3$, n-But and MeOH extracts (especially at highest concentration) while no activity with n-Hex fraction. The n-But extract showed the highest activity of 18.50±0.41 at 100mg/ml, followed by CHCL3 (10.00±2.12) and MeOH (8.166±0.62) respectively; but however, lower than that of the control vancomycin (25.00±1.3) (Table1). This demonstrate that the active antimicrobial contents of the root of *G.kola* are from the polar/non-polar intermediate solvents. This is consonant with the finding of Idu and colleagues on the $CHCl_3$ root extract activity of *G.kola* on staph aureus (Idu *et al*., 2014).

Subsequent analysis of the most active extract; n-But was performed with a GC-MS. 14 different phytoconstituents with varying structural and physicochemical properties were obtained (Table 2). Their PubChem ID, molecular weight, IUPAC name, formula and retention time are also given (Table 2). Some of the compounds exhibit benzoquinone, imidazo[1,2-a]pyridine, Chlorocarbazole and azetidine scaffolds & motifs. Presence of this moieties in a compound attributes to its biological activity including potent antibacterial activity. Thus, the antibacterial activity exhibited by the n-But extracted is due to these compounds.

To investigate this claim, an *insilico* studies was performed with these compounds and results documented; the physiochemical analysis of drug likeness and Lipinski's rule of five (LO5) (Table 3) and molecular docking analysis against *Staph. aureus* tyrosyl-tRNA synthatase; a *Staph. aureus* bacterial drug target that is implicated in protein synthesis (Table 4). The results showed the compounds to possess good physiochemical and drug likeness score. In the molecular docking analysis, compound CID_619544, CID_619583, CID_5732, CID_616643, CID_622021, CID_616496, CID_590350 and CID_16486 showed good binding score of -4.63 to -7.08 kcal/mol against the target protein and exhibit varying H-bond interaction.

DoGSiteScorer was used to predict the binding pockct of the ligand. It employs the grid-based method that utilize the Difference of Gaussian filter to detect potential binding pockets solely based on the 3D structure of the protein; values are between zero and one and the higher the score the more druggable the pocket is estimated to be (Volkamer *et al*., 2012). Model interaction of the Protein- ligand is also analyzed and 2D structure generated with PoseViewer. TyrRS is characterized by a α-helical domain, linked to the catalytic domain, and a C-terminal domain. The catalytic domain contains a six-stranded parallel β-sheet and a deep active-site cleft (Qui *et al*., 2020). The authors also described the potential binding sides of inhibitors of TyrS; tyrosine, tyrosyl-AMP, ribose and tyrosinyl-adenylate complex.

CID_619544 had a binding score of -4.63 kcal/mol. It forms a two H bonding residues with the protein target. A terminal OH of Thr169 (2.97 **Å** and 3.02 **Å**) with the carbonyl and OH of the benzoquinone ring. Π interaction are seen with Phe136, Leu173 and Leu128, likewise, also Vander waals interaction (Fig 1). The compound occupies a binding space with a Vol 242.18 A^3, Surface area 250.61 A^2 and Drug score 0.45. This compound contains a 1,4-benzoquinone moiety, which are essential structural units of quinones compounds. Many natural derivatives had been isolated and synthesized, with potent antimicrobial activities documented (Abraham *et al*., 2011).

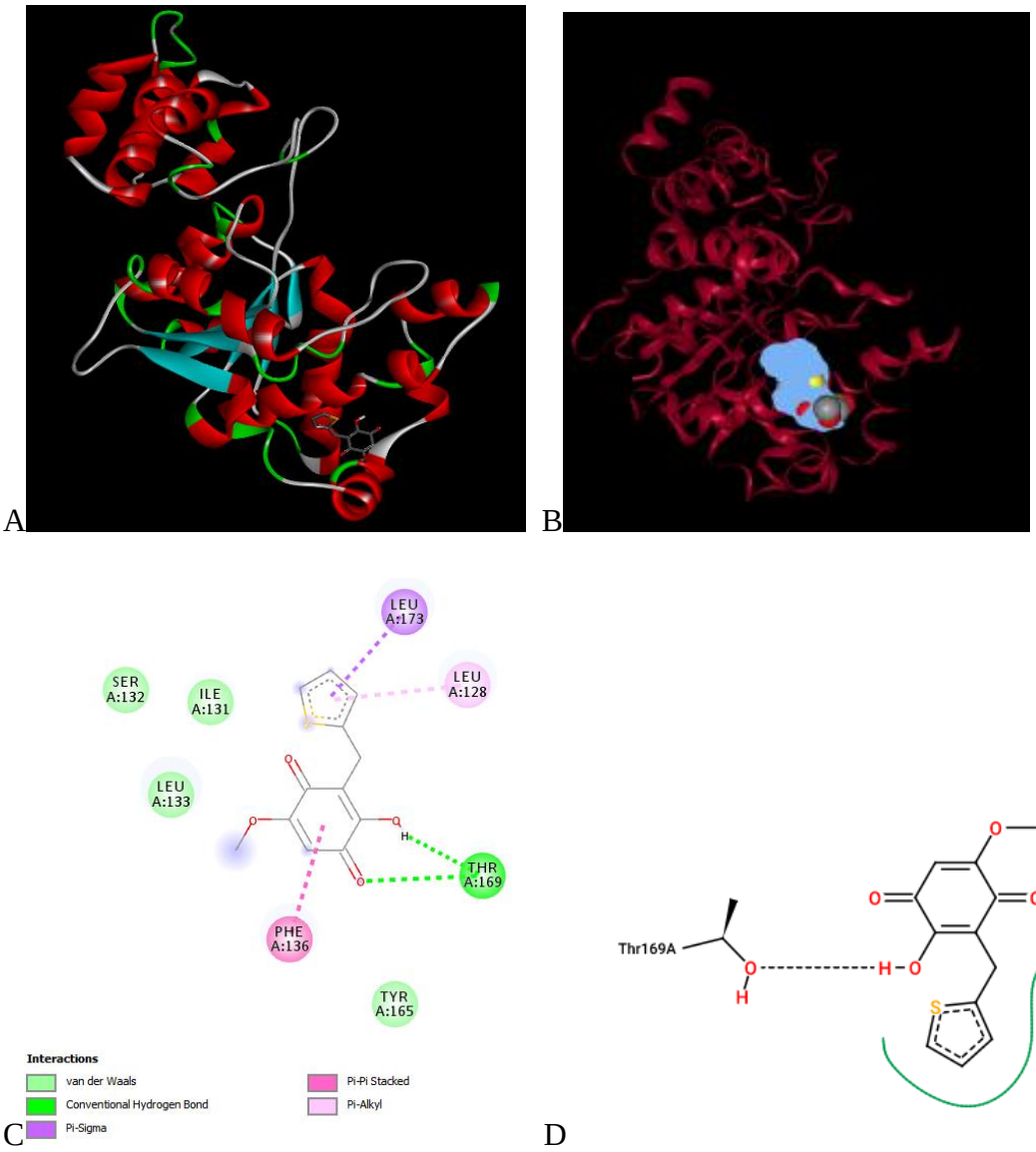

Fig 1: 2-Hydroxy-3-(thiophen-2-yl)methyl-5-methoxy-1,4-benzoquinone. **A**-protein-ligand complex. **B**-Ligand Binding Domain (LBD). **C and D**- 2D interaction model of CID_619544 and 1JIJ.

CID_619583 with a binding score of -5.91kcal/mol forms no H-bond interaction, but weak van der waals interaction are seen with the amino acid residues of PDB 1JIJ (Fig2). There's also a π-alkyl interaction of Leu173, Leu128 and Ile78 with the diphenyl ring of CID_619583 (Fig2). The compound binds to a different pocket not predicted by the DoGSiteScorer (Fig2)

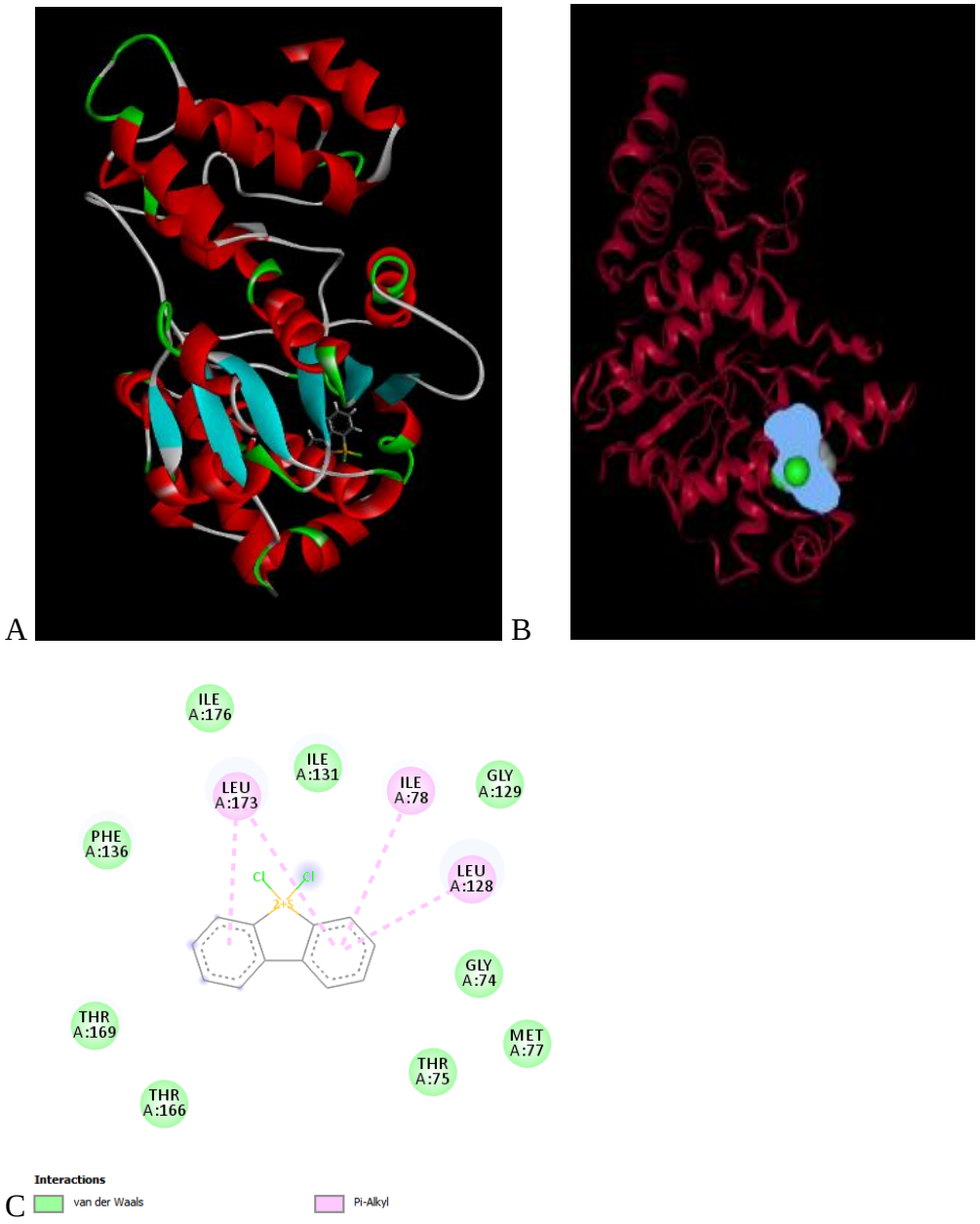

Fig 2: 9,9-Dichloro-9-silafluorene A-protein-ligand complex. B-Ligand Binding Domain (LBD). C - 2D interaction model of CID_619583 and 1JIJ.

CID_5732 with a binding score of 6.03 kcal/mol also doesn't forms H-bond with 1JIJ, but various π interaction including a π - π Phe136 and π -sigma Leu133 with the 4-tolyl group at position 2. Van der Waals interaction are also seen with imidazo[1,2-a]pyridine moeity (Fig3). It binds and occupies in the active binding pocket with a Vol 242.18 A^3, surface area 350.61 A^2

and Drug score 0.45 (Fig3). The imidazo[1,2-a]pyridine presents as an important scaffold in medicinal chemistry for development of active molecules. Many drugs had been designed to contain this active moiety including the antibiotic Rifaximin (Nisha *et al*., 2016).

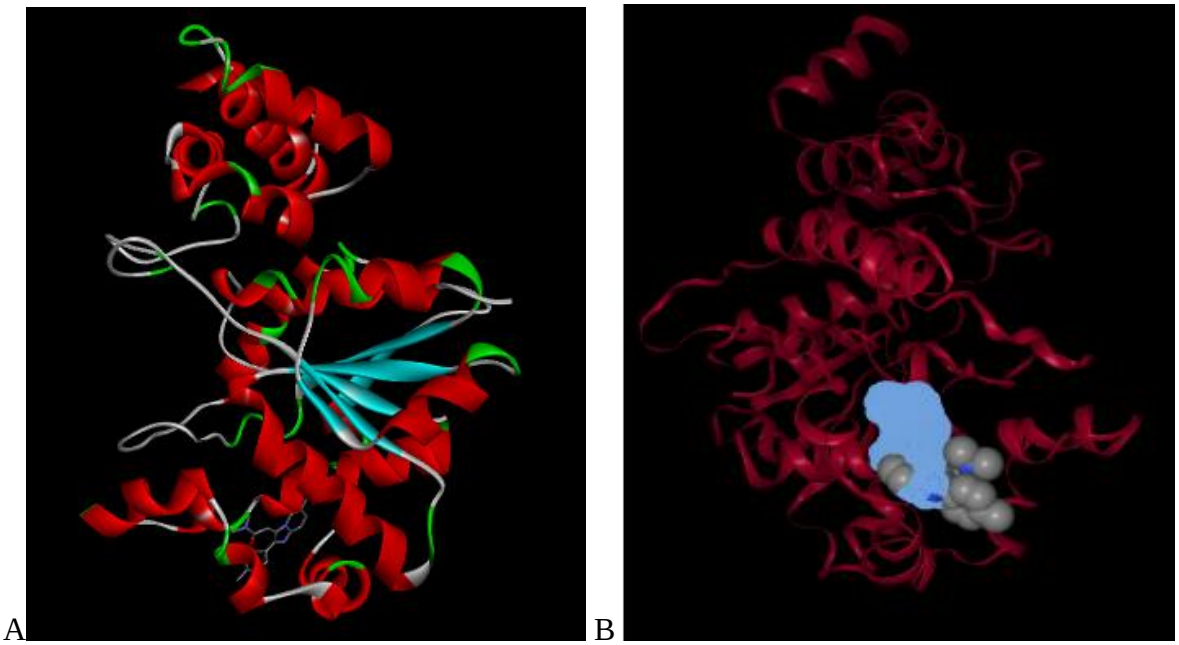

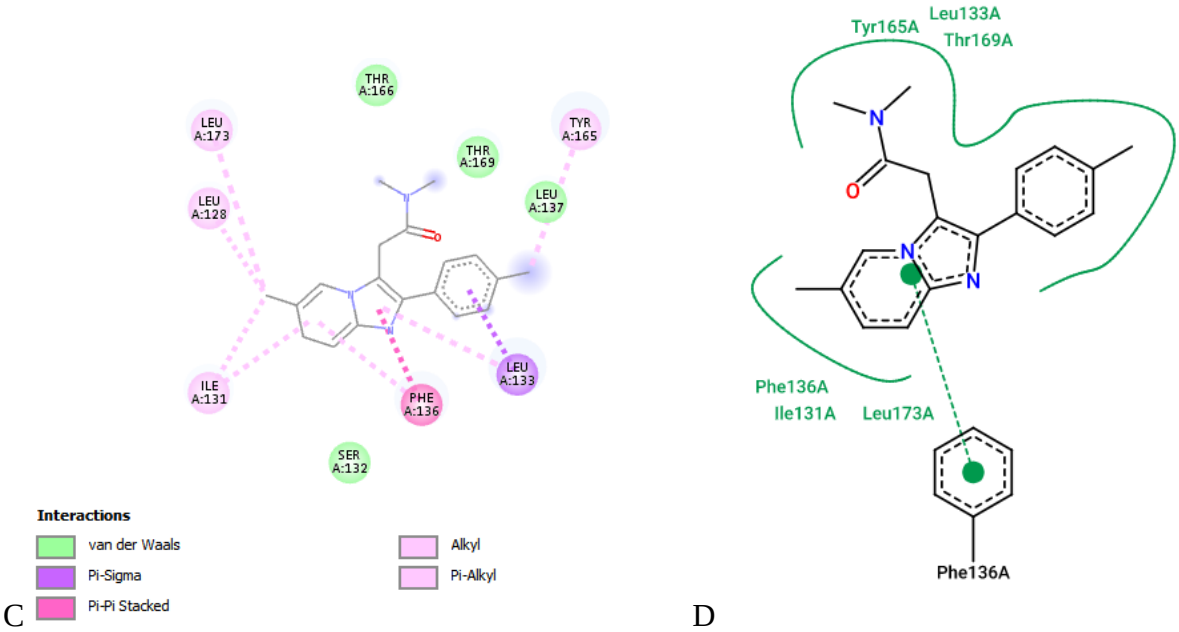

Fig 3: Zolpidem. A-protein-ligand complex. B-Ligand Binding Domain (LBD). C and D- 2D interaction model of CID_5732 and 1JIJ.

CID_616643 is a pyridazinedicarbonitrile derivative. It has a binding score of -5.62kcal/mol and forms two H-bond interaction with 1JIJ (Table). A binding of Tyr165 (3.02 **Å)** terminal OH with the 3,5-carbonitryl moiety at position 3 and terminal OH of Thr169 (2.72 **Å)** with the 2-nitrophenyl moiety. Van der Waals interaction are seen with Ile131, Ser132, Leu173 & Leu137. Similarly, π- π interaction of Leu133 with Pyridazine-3,5-dicarbonitrile moiety and a Phen136 π –sigma interaction with the 2-nitrophenyl ring (Fig4). The compound binds at an active binding pocket in the target with a Vol 243.18 A^3, Surface 350.61 A^3 and Drug score 0.45.

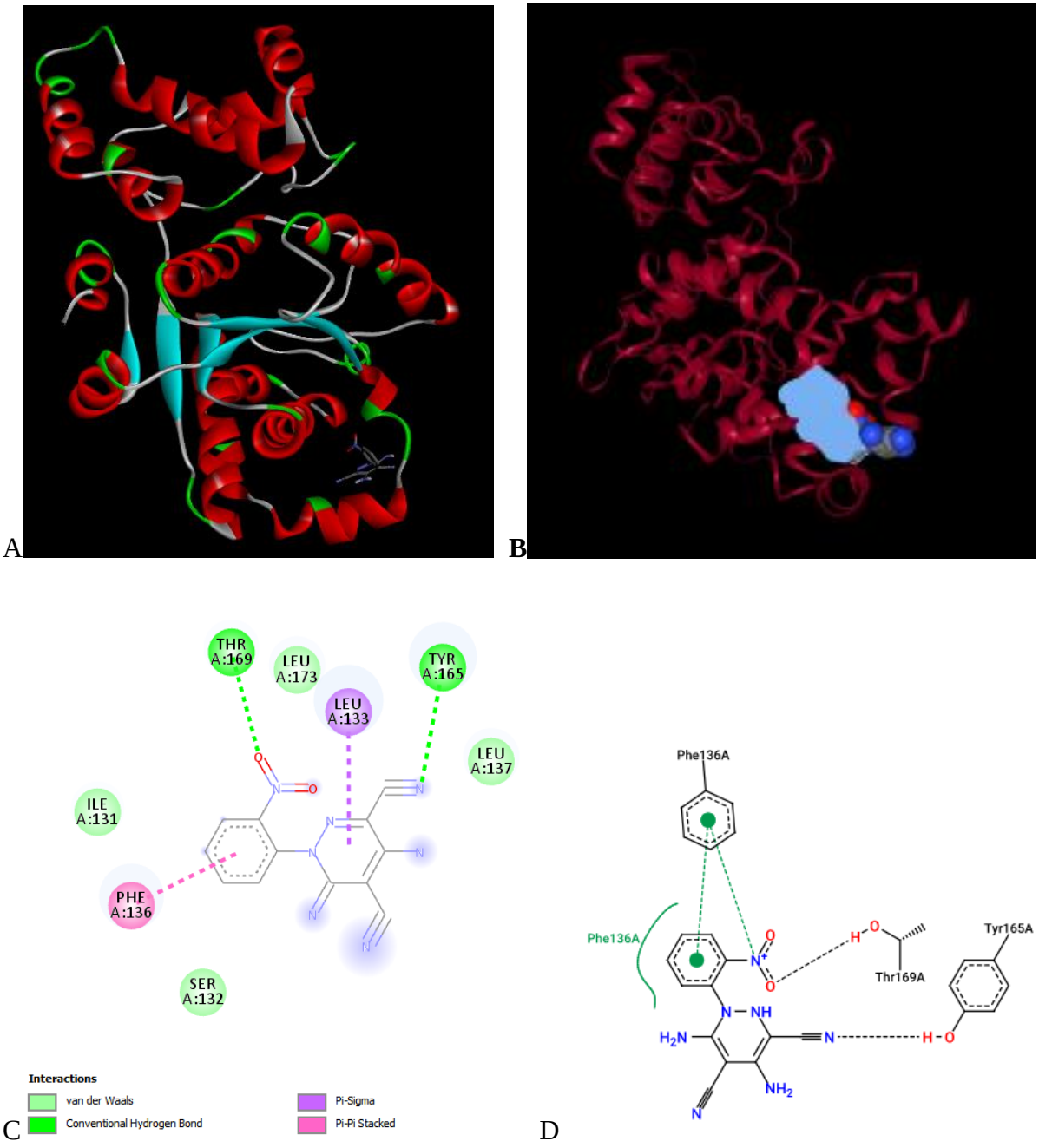

Fig 4: Pyridazine-3,5-dicarbonitrile, 1,6-dihydro-4-amino-6-imino-1-(2-nitrophenyl)-. A-protein-ligand complex. B-Ligand Binding Domain (LBD). C and D- 2D interaction model of CID_616643 and 1JIJ.

CID_622021 has a binding score of -7.01kcal/mol (Table) and forms only one H-bond with residues of 1JIJ (Fig5). A terminal carbonyl C=O of the 5H-Naphtho ring with the terminal OH of Thr169 (3.06 **Å)** residue. Van der Waal and π interaction are also observed (Fig5).

The compound binds in the protein target binding site with a Vol 242.18 A^3, Surface area 350.61 A^2 and Drug score 0.45.

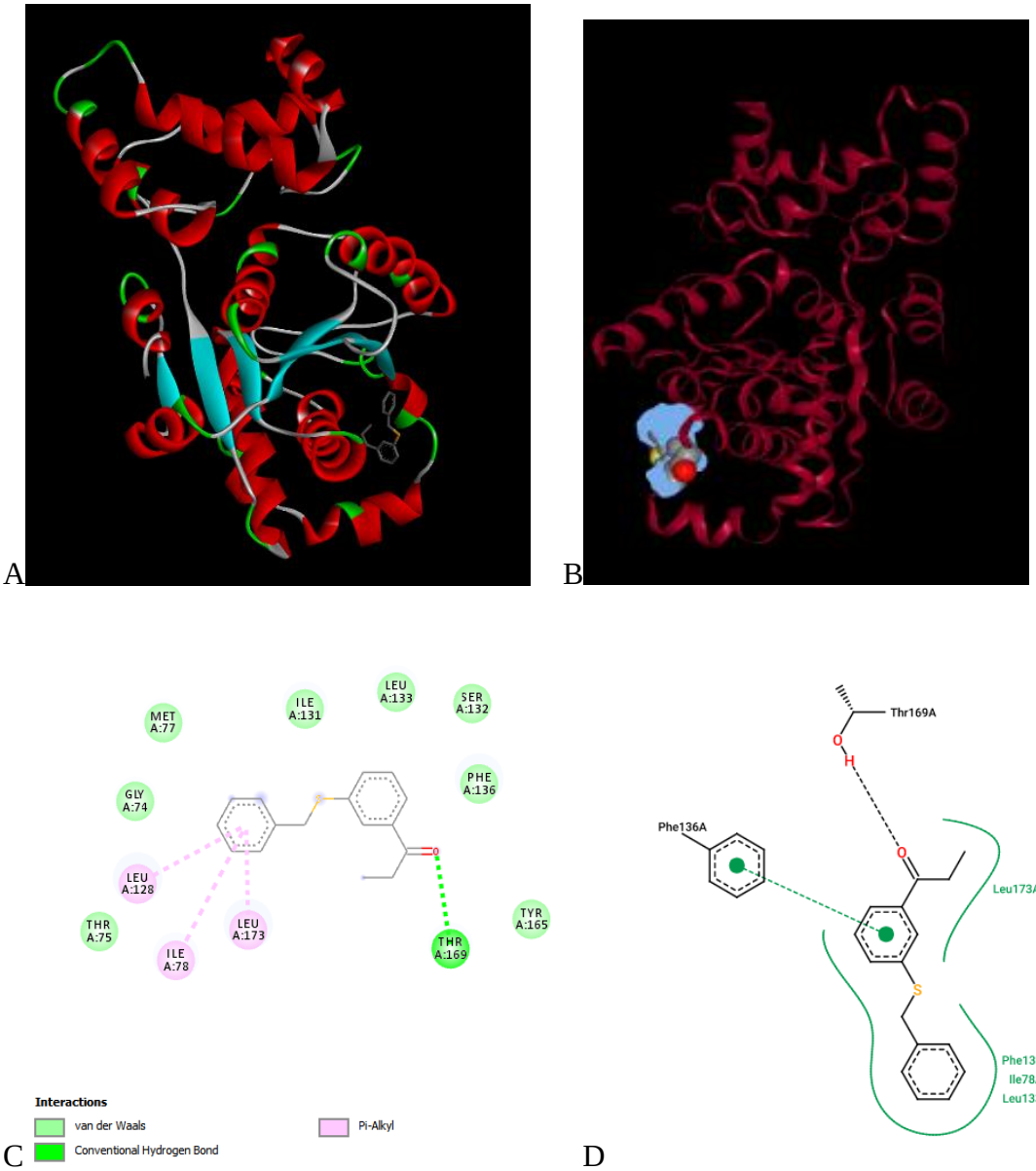

Fig 5: 5H-Naphtho[1,8-bc]thiophen-5-one, 3,4-dihydro-2-phenyl-. A-protein-ligand complex. B-Ligand Binding Domain (LBD). C and D- 2D interaction model of CID_622021 and 1JIJ.

CID_616496 is a dichlorocarbazole derivative. A binding score of -7.0 kcal/mol was recorded and forms no H-bond with 1JIJ (Tab 4). A van der Waal interaction is seen with CID_616496; Ile78, Ile172, Thr166 & Gly141. Likewise π interactions including π- π bond with Phe136 and π-sigma bond with Leu133 residues respectively (Fig 6). The compound doesn't occupies completely a position predicted of an active binding pocket, however, its occupies partially in a site in close proximity with a binding site with Vol 176.58 A^3, Surface area 389.51 A^2 and Drug score of 0.34

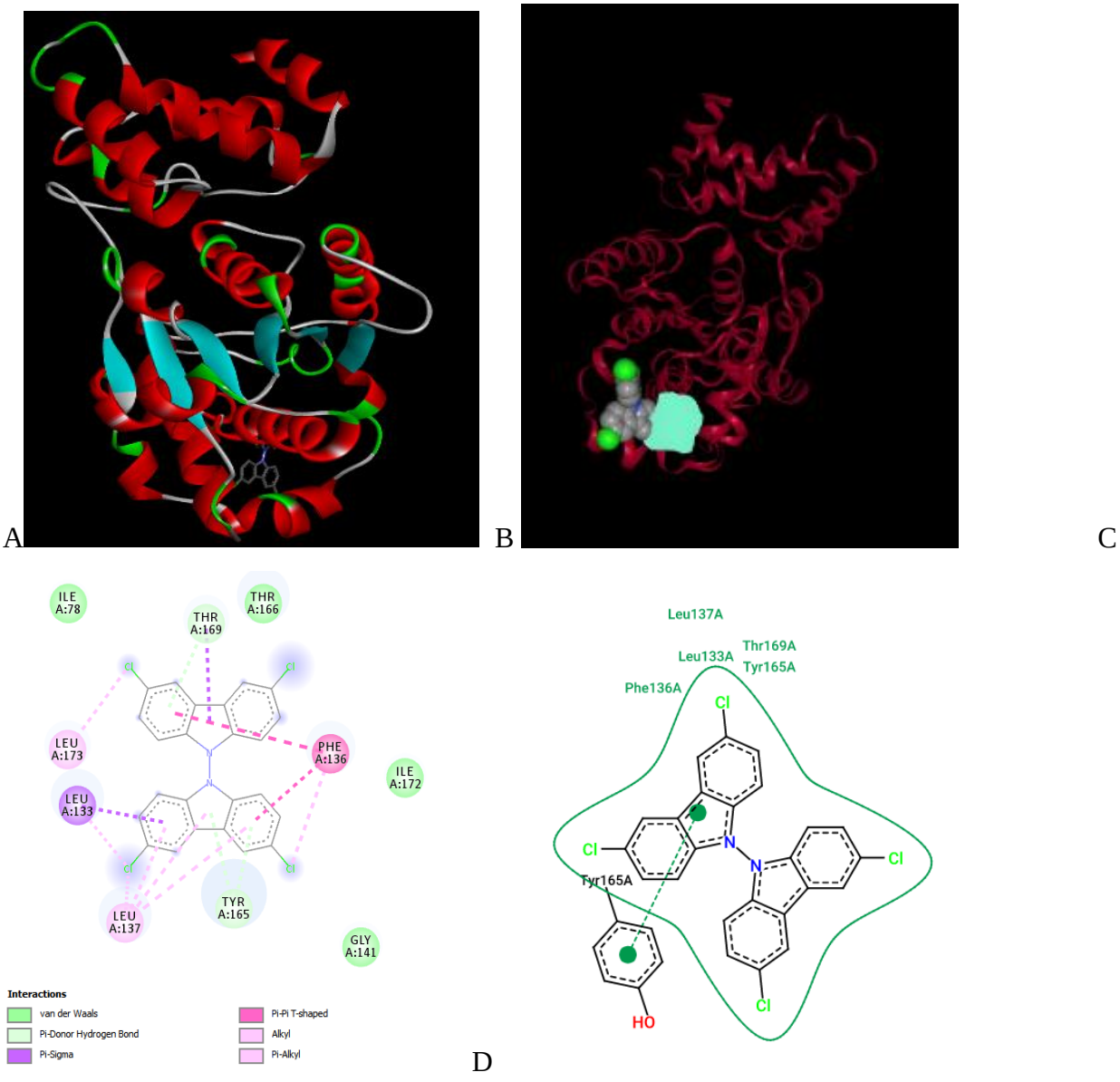

Fig 6: 9,9'-Bis(3,6-dichlorocarbazole) A-protein-ligand complex. B-Ligand Binding Domain (LBD). C and D- 2D interaction model of CID_616496 and 1JIJ.

CID_590350 occupies partially a binding pocket site with Vol 242.18 A^3, Surface area 350.61 A^2 and Drug score of 0.45. it recorded a binding score of -7.08 kcal/mol and also forms no H-bond with 1JIJ residues (Tab 4). Thr169, Thr166, Ile78, Ser132 and Ile131 all form weak van der Waal interaction with CID_590350. A π-π interact is seen with Try165 (Fig 7).

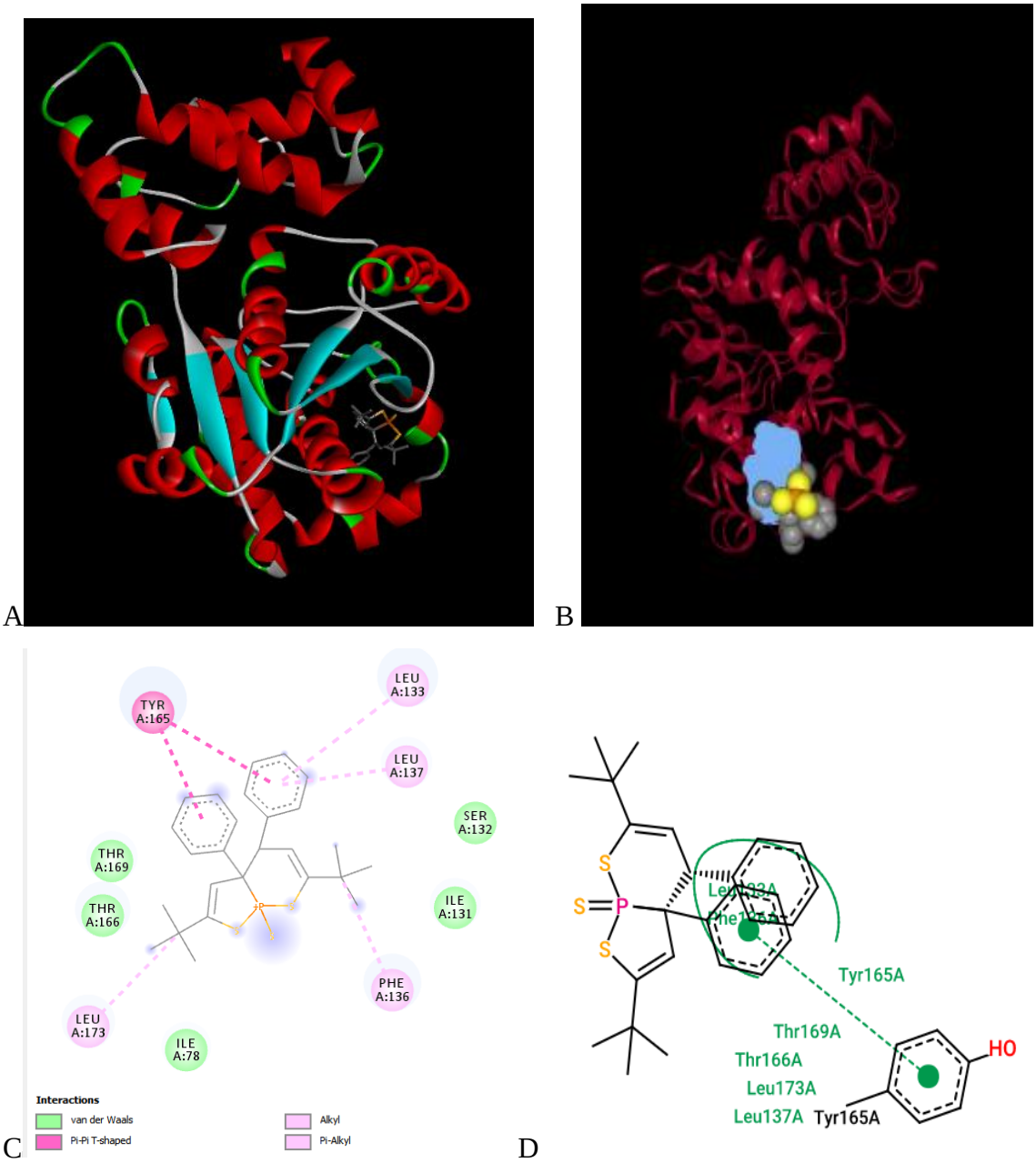

Fig 7: 3,8-Di-t-butyl-5,6-diphenyl-2,9-dithia-1-phosphabicyclo[4.3.0]nona-3,7-diene 1-sulfide. A-protein-ligand complex. B-Ligand Binding Domain (LBD). C and D- 2D interaction model of CID_590350 and 1JIJ.

CID_16486 is an aliphatic heteromonocyclic compound. It's a natural azetidine derivative produced by plant as a protective agent against predators like insects. In this study, the compounds binds to the most active site of the binding pocket with a Vol 916.61A^3, Surface area 894.72A^2 and Drug score of 0.82. The binding score was -4.64 kcal/mol and forms five H-bonding with residues of 1JIJ (Tab 4). Theres a H_3-N and HN interaction of Lys84 (2.67 Å) and Asp80 (2.98 Å) respectively with the –COO^- group of CID_16486. Likewise an amino H_2-N with the terminal –COO^- of Asp40 (2.88 Å). Other H-bond interaction include that of Tyr170 (3.03 Å) and Arg88 (2.85 Å), while van der Waals interaction are also seen (Fig 8). A

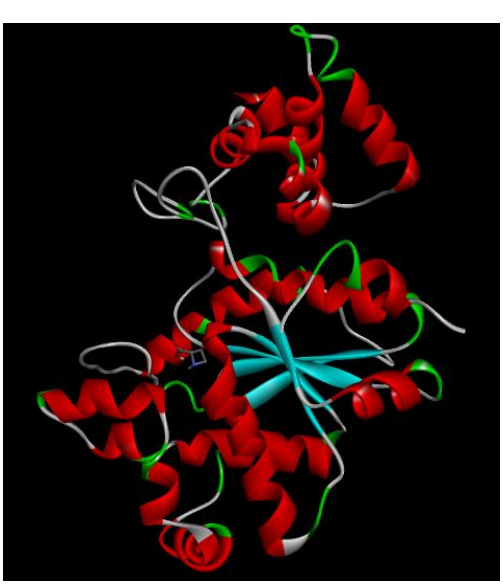

B

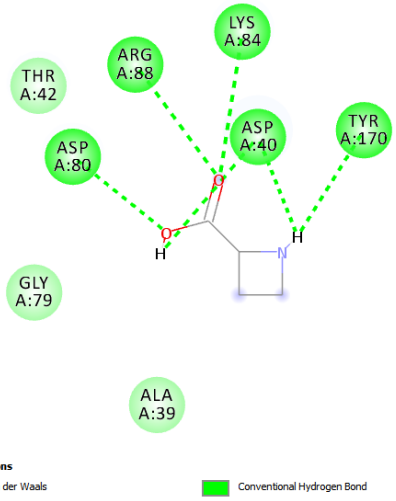

C

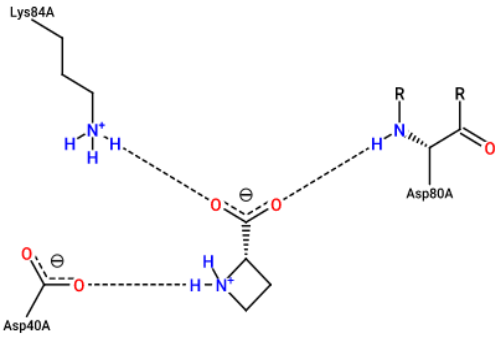

D

Fig 8: (S)-azetidine-2-carboxylic acid. A-protein-ligand complex. B-Ligand Binding Domain (LBD). C and D- 2D interaction model of CID_16486 and 1JIJ.

These compounds are non proteinogenic amino acid homologue of proline, making them proline antagonist. This features make them potent antibiotics. Since then, a number of both natural product and synthetic compounds having this amino acid moiety had been isolated and synthesize, offering a variety of Pharmaceutical compounds including the antibiotic polyoxin(s) (Couty and Evano, 2006).

CID_66747 is a benzoate derivatives and also binds to one of most active site of the binding pocket with a Vol 250.3 A^3, Surface area 413.0 A^2 and Drug score of 0.72. It recorded a binding score of -4.93 kcal/mol and forms two H-bond residues (Tab). The carboxylic $–COO^-$ of Glu205 (2.99 Å) with the 2-OH group of CID_66747 and Leu206 with the benzoate moiety of CID_66747. Associated van der Waals and π interactions are also witnessed (Fig 9).

A 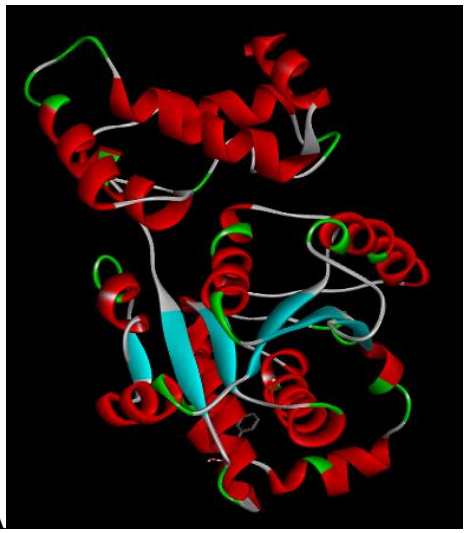

B 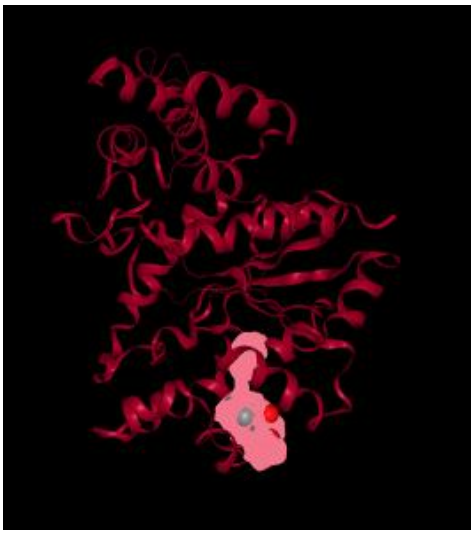

C 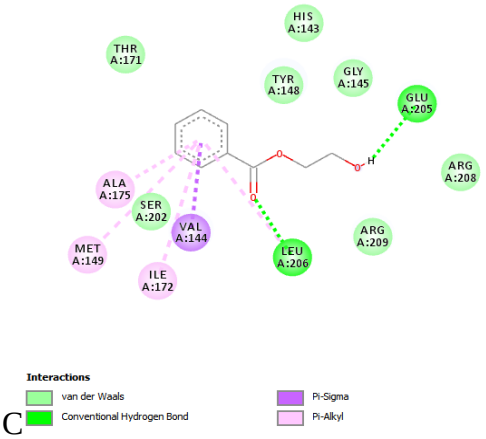

D 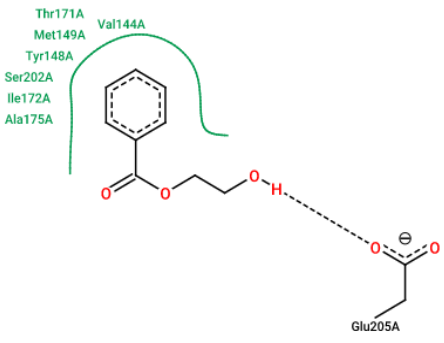

Fig 9: 2-hydroxyethyl benzoate. A-protein-ligand complex. B-Ligand Binding Domain (LBD). C and D- 2D interaction model of CID_66747 and 1JIJ.

CONCLUSION

The root extracts of *Garcinia kola* showed promising activity against MDR *Staphylococcus aureus.* The n-Butanol fraction recorded the highest activity; 18.50±0.41 and its phytoconstituents were explored using GC-MS analysis. A Total of 14 compounds were obtained and subjected to physicochemical analysis and insilico molecular docking studies; which determine their binding energies with *Staphylococcus aureus* tyrosyl-tRNA synthetase (PDB 1JIJ). The result of the docking studies showed that 9 compounds; CID_619544, CID_619583, CID_5732, CID_616643, CID_622021, CID_ 616496, CID_590350, CID_16486 and CID_66747 had good binding scores ranging from -4.63 to -7.08 kcal/mol; with CID_590350 having the highest score. Further analysis for Pharmacokinetic parameters was recorded. Thus, these compounds from *G.kola* are proposed to be potential inhibitors of tyrosyl-tRNA synthetase and effective against MDR *Staphylococcus aureus* after successful experimental validation.

REFERENCE

Steinig, E. J., Duchene, S., Robinson, D. A., Monecke, S., Yokoyama, M., Laabei, M., … Tong, S. Y. C. (2019). *Evolution and Global Transmission of a Multidrug-Resistant, Community-Associated Methicillin-Resistant Staphylococcus aureus Lineage from the Indian Subcontinent. mBio, 10(6).* doi:10.1128/mbio.01105-19

Hiramatsu K, Katayama Y, Matsuo M, Sasaki T, Morimoto Y, Sekiguchi A, Baba T. Multi-drug-resistant Staphylococcus aureus and future chemotherapy. J Infect Chemother. 2014 Oct;20(10):593-601. doi: 10.1016/j.jiac.2014.08.001. Epub 2014 Aug 27. PMID: 25172776.

Anstead, G. M., Cadena, J., & Javeri, H. (2013). Treatment of Infections Due to Resistant Staphylococcus aureus. Methicillin-Resistant Staphylococcus Aureus (MRSA) Protocols, 259–309. doi:10.1007/978-1-62703-664-1_16

Othman L, Sleiman A and Abdel-Massih RM (2019) Antimicrobial Activity of Polyphenols and Alkaloids in Middle Eastern Plants. Front. Microbiol. 10:911. doi: 10.3389/fmicb.2019.00911

Ferdes, Mariana. (2018). Antimicrobial compounds from plants. 10.5599/obp.15.15. In book: Fighting Antimicrobial Resistance, Edited by Ana Budimir, http://iapc-obp.com/books/release_detail/15 (pp.243-271) Chapter: Antimicrobial Compounds from plants (pages 273-271) Publisher: IAPC-OBP, Zagreb, Croatia

Khameneh, B., Iranshahy, M., Soheili, V. et al. Review on plant antimicrobials: a mechanistic viewpoint. Antimicrob Resist Infect Control **8,** 118 (2019).

Osuntokun, Oludare & Ige, Olufola & Gamberini, Maria & Idowu, Thomas. (2018). Bio-activity and Spectral Analysis of Gas Chromatography/Mass Spectroscopy (GCMS) Profile of Crude Spomdias mombin Extracts. Analytical Biochemistry. 2. https://doi.org/10.1186/s13756-019-0559-6

Devi, Nisha & Singh, Dharmender & Rawal, Ravindra & Bariwal, Jitender & Singh, Virender. (2016). Medicinal Attributes of Imidazo[1,2-a]pyridine Derivatives: An Update. Current topics in medicinal chemistry. 16. 10.2174/1568026616666160506145539.

Couty, F., & Evano, G. (2006). AZETIDINE-2-CARBOXYLIC ACID. FROM LILY OF THE VALLEY TO KEY PHARMACEUTICALS. A JUBILEE REVIEW. Organic Preparations and Procedures International, 38(5), 427–465. doi:10.1080/00304940609356436

Volkamer, D. Kuhn, T. Grombacher, F. Rippmann, M. Rarey. Combining global and local measures for structure-based druggability predictions. J. Chem. Inf. Model. 2012,52,360-372

Abraham, Ignatious, Joshi, Rahul, Pardasani, Pushpa, & Pardasani, R.T. (2011). Recent advances in 1,4-benzoquinone chemistry. Journal of the Brazilian Chemical Society, 22(3), 385-421. https://dx.doi.org/10.1590/S0103-50532011000300002

Daina, A., Michielin, O. & Zoete, V. SwissADME: a free web tool to evaluate pharmacokinetics, drug-likeness and medicinal chemistry friendliness of small molecules. *Sci Rep* **7,** 42717 (2017). https://doi.org/10.1038/srep42717

Qiu, X., Janson, C. A., Smith, W. W., Green, S. M., McDevitt, P., Johanson, K., Carter, P., Hibbs, M., Lewis, C., Chalker, A., Fosberry, A., Lalonde, J., Berge, J., Brown, P., Houge-Frydrych, C. S., & Jarvest, R. L. (2001). Crystal structure of Staphylococcus aureus tyrosyl-tRNA synthetase in complex with a class of potent and specific inhibitors. *Protein science : a publication of the Protein Society*, *10*(10), 2008–2016. https://doi.org/10.1110/ps.18001

Chiako Farshadfar, Adriano Mollica, Fatemeh Rafii, Akbar Noorbakhsh, Mozhgan Nikzad, Seyed Hamid Seyedi, Fatemeh Abdi, Somayeh Abbasi Verki & Sako Mirzaie (2020) Novel potential inhibitor discovery against tyrosyl-tRNA synthetase from *Staphylococcus aureus* by virtual screening, molecular dynamics, MMPBSA and QMMM simulations, Molecular Simulation, 46:7, 507-520, DOI: 10.1080/08927022.2020.1726911

Indabawa, I.I and Arzai, A.H. (2011). Antibacterial activity of Garcinia kola and Cola nitida seeds extracts. *Bayero Journal of Pure and Applied Sciences.* Vol. 4 No. 1 (2011). **DOI:** 10.4314/bajopas.v4i1.11

Ajayi T. O , Moody J.O , Fukushi Y , Adeyemi T.A , Fakeye T.O. (2014). Antimicrobial Activity of Garcinia kola (Heckel) Seed Extracts and Isolated Constituents Against Caries-causing Microorganisms Afr. J. Biomed. Res. Vol.17; 165- 171 .

John, O. Akerele, Osahon, Obasuyi , Maureen, I. Ebomoyi Israel, E. Oboh , Osamuyi, H. Uwumarongie (2008). Antimicrobial activity of the ethanol extract and fractions of the seeds of Garcinia kola Heckel (Guttiferae). African Journal of Biotechnology Vol. 7 (2), pp. 169-172, 18 January, 2008.

C. I. Buba, S. E. Okhale and I. Muazzam. GARCINIA KOLA: THE PHYTOCHEMISTRY, PHARMACOLOGY AND THERAPEUTIC APPLICATIONS.No 2: 67-81.
DOI: 10.13040/IJPSR.0975-8232.IJP.3(2).67-81

MacDonald Idu, Nosa O. Obayagbona, Emmanuel O. Oshomoh , Joseph O. Erhabor (2014) Phytochemical and Antimicrobial Properties of Chrysophyllum albidum, Dacryodes edulis, Garcinia kola chloroform and ethanolic root extracts. *Journal of Complementary Medicine Research,* 3 (1), 15-20. doi:10.5455/jice.20140109033957

Pisano, M. B., Kumar, A., Medda, R., Gatto, G., Pal, R., Fais, A., Era, B., Cosentino, S., Uriarte, E., Santana, L., Pintus, F., & Matos, M. J. (2019). Antibacterial Activity and Molecular Docking Studies of a Selected Series of Hydroxy-3-arylcoumarins. *Molecules (Basel, Switzerland), 24*(15), 2815. https://doi.org/10.3390/molecules24152815

Kot, B., Wierzchowska, K., Piechota, M., & Grużewska, A. (2019). *Antimicrobial Resistance Patterns in Methicillin-Resistant Staphylococcus aureus from Patients Hospitalized during 2015 - 2017 in Hospitals in Poland. Medical Principles and Practice.* doi:10.1159/000501788

Yakubu, Abdulbasit Haliru; Mohammed, Mohammed Mustapha; bababe, Abdulqadir bukar; Yesufu, Hassan (2020): Phytochemical Screening, Antioxidant and Antibacterial Activity of the Root Extract of Cyphostemma Adenocaule (Steud. Ex A. Rich.) Wild & R.B.Drumm. ChemRxiv. Preprint. https://doi.org/10.26434/chemrxiv.13296389.v1

Tcheghebe, Olivier & Signe, Martin & Seukep, Armel Jackson & Tatong, Francis. (2016). Review on traditional uses, phytochemical and pharmacological profiles of Garcinia kola Heckel. Merit Research Journal of Medicine and Medical Sciences. 4. 480-489.